Why does a spinning egg rise?

Why does a spinning egg rise?

Rod Cross

School of Physics, University of Sydney, Sydney, Australia

email: rodney.cross@sydney.edu.au

Abstract

Experimental and theoretical results are presented concerning the rise of a spinning egg. It was found that an egg rises quickly while it is sliding and then more slowly when it starts rolling. The angular momentum of the egg projected in the XZ plane changed in the same direction as the friction torque, as expected, by rotating *away* from the vertical Z axis. The latter result does not explain the rise. However, an even larger effect arises from the Y component of the angular momentum vector. As the egg rises, the egg rotates about the Y axis, an effect that is closely analogous to rotation of the egg about the Z axis. Both effects can be described in terms of precession about the respective axes. Steady precession about the Z axis arises from the normal reaction force in the Z direction, while precession about the Y axis arises from the friction force in the Y direction. Precession about the Z axis ceases if the normal reaction force decreases to zero, and precession about the Y axis ceases if the friction force decreases to zero.

1. Introduction

The precession of a spinning top is not easy to explain in simple terms, but it helps to recognise that the change in angular momentum of a spinning top is in the same direction as the gravitational torque acting on the top. Instead of falling down, as one might intuitively expect, a spinning top moves sideways by precessing slowly around a vertical axis through the bottom end of the top. If the top spins fast enough, it can rise to a sleeping position where the spin axis is vertical and the top stops precessing. In both of these respects, a rapidly spinning top defies gravity by moving upwards and sideways rather than falling downwards.

A similar and even more surprising result is observed if a hard-boiled egg is spun rapidly on a horizontal surface. If the long axis of the egg is initially horizontal, or approximately horizontal, then the egg rises to spin on one end. While the egg is rising it rotates rapidly about a vertical axis that passes through or close to the center of mass. If the egg is spun fast enough it can rise to a sleeping position with its long axis vertical, otherwise it rises to a point where the long axis is inclined away from the vertical and the egg then continues to precess about the vertical axis without any further rise.

The rise of a spinning egg [1-7], or a spinning top [8-16], or a tippe top [17-20] is commonly explained in terms of the horizontal friction force acting at the bottom end. The explanations

usually involve solutions of a relatively complex set of equations, in which case the essential physics of the problem tends to be obscured. The essential physics cannot be conveyed to an undergraduate student or to a physics teacher by explaining that an egg rises because the equations predict that it will rise.

The object of the work described in present paper was to measure the rise of a spinning egg in an attempt to find a simple physical explanation for the rise in terms of the forces and torques acting on the egg. The rise and precession of a spinning top can easily be explained in this manner, but the same explanation cannot easily be given for the rise and precession of a spinning egg. The main difference is that the precession frequency of a top is generally much smaller than the spin frequency, whereas the precession frequency of a spinning egg is initially much larger than the spin about the long axis of the egg. As a result, the angular momentum vector of a spinning top points closely along the axis of the top, whereas it points closely to the vertical for a spinning egg. Nevertheless, the change in angular momentum of a top or an egg must be in the same direction as the applied torque.

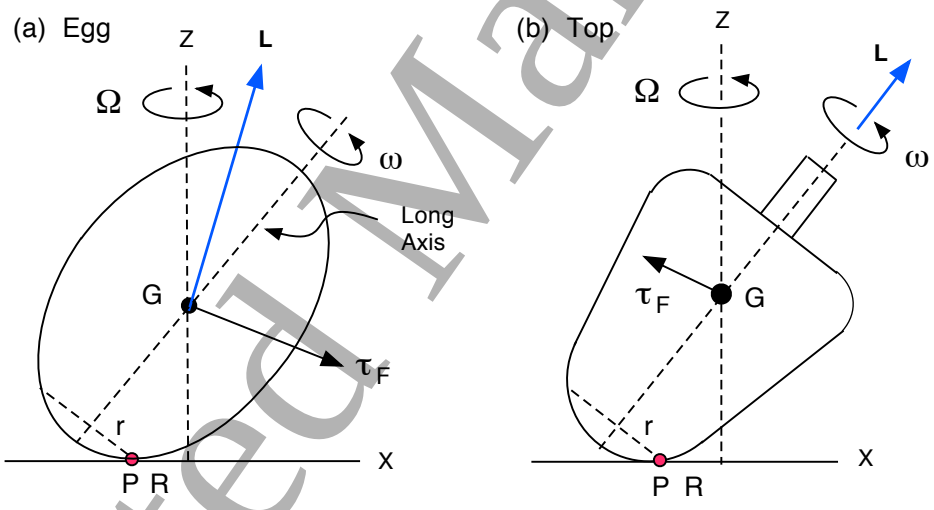

FIG. 1: Diagrams showing (a) an egg and (b) a top, each spinning at angular velocity, ω, about the long axis and precessing at angular velocity, Ω, around a vertical axis through the center of mass, G. The friction force, F, acts into the page in (a) since Ω is initially much larger than ω, so the torque due to F, τ_F, points down to the right, and the angular momentum vector $\mathbf{L}$, rotates down towards the horizontal surface. In (b), F acts out of the page since $\omega \gg \Omega$, so τ_F points up to the left, and $\mathbf{L}$ rotates towards the vertical.

At first sight, the friction torque on an egg appears to act in the wrong direction. Suppose

that an egg is spinning about its long axis at angular velocity, ω, and is rotating about a vertical axis at angular velocity, Ω, as indicated in figure 1(a). If the egg is spinning rapidly then the spin and the precession are in the same directional sense, and are observed to be similar in magnitude when the egg is inclined more than about thirty degrees above the horizontal. The torque about the center of mass, G, due to the normal reaction force is directed into the page, with the result that the top end of the egg precesses by rotating into the page. Assuming that G rises slowly as the egg rises, the bottom end of the egg precesses by rotating out of the page. That is, the egg precesses in a counter-clockwise direction when viewed from above. The change in the angular momentum in this case is in the same direction as the torque about the center of mass, as expected.

In figure 1(a), the contact point on the egg can slide out of the page or into the page, or it can roll along the surface, depending on the relative magnitudes of $R\,\Omega$ and $r\omega$, where R is the horizontal distance of the contact point, P, from the vertical axis through G, and r is the perpendicular distance from the contact point to the long axis. When the egg is initially spun with its long axis approximately horizontal, $R\,\Omega$ is much larger than $r\omega$ so the contact point slides out of the page and the friction force acts into the page. The friction torque about the center of mass therefore points downwards to the horizontal surface. The angular momentum vector will therefore rotate in that direction (while simultaneously precessing about the vertical axis) and the egg might be expected to rotate or precess downwards rather than to rise.

An analogous problem is encountered in relation to spinning tops, as indicated in figure 1(b). A rapidly spinning top with a rounded peg can also rise into a sleeping position. However, the precession frequency of a spinning top is typically much smaller than the spin frequency, in which case the contact point of the peg slides into the page as a result of its rapid spin motion even though the peg moves slowly out of the page due to the precessional motion of the top. The friction force on a spinning top therefore acts in the opposite direction to the friction force on a spinning egg. The rise of a spinning top can be explained simply in terms of the direction of the friction torque and the corresponding rotation of the angular momentum vector in an upwards direction. How then can we explain the rise of a spinning egg?

In this paper, an experiment is described where the precession frequency, the direction of the friction force and the direction of the angular momentum were measured for three

spinning spheroids. The author could find no other similar measurements in the literature. A spheroid is similar in shape to an egg but is elliptical in cross section and its center of mass is at an equal distance from each end. It was found that after the initial rapid rise phase while the spheroid was sliding, the spheroid started to roll and then precessed in a steady manner for about ten seconds before it eventually fell. It was also found that a slowly spinning spheroid or a spinning egg can precess at two different frequencies simultaneously, as noted previously [21].

2. Theoretical model of a spinning egg

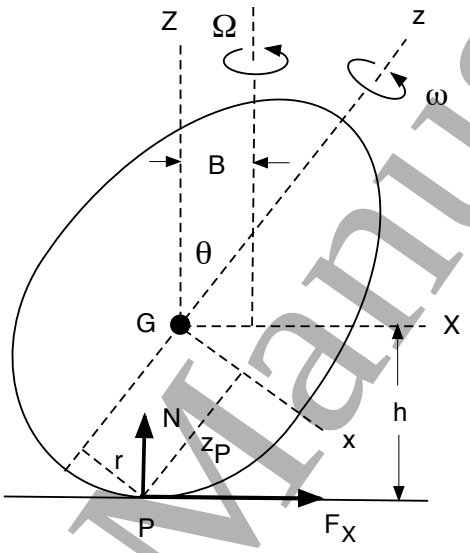

FIG. 2: An egg spinning at angular velocity, ω, about its long axis and precessing at angular velocity, Ω, around a vertical axis displaced horizontally from the center of mass, G. The long axis is inclined at angle θ to the vertical. Two rotating coordinate systems are used, one (XYZ) with vertical and horizontal axes, the other (xyz) being rotated by angle θ from the first so that the z axis lies along the long axis. N is the normal reaction force at the contact point, P. Horizontal friction forces F_X and $F_y = F_Y$ also act at P.

Theoretical descriptions of the behaviour of spinning eggs have been presented previously [1-5]. We summarise here the main results of interest and extend the results to include the experimental observation that an egg (or a spheroid) can precess about a vertical axis displaced horizontally by a distance B from the center of mass, G. The geometry is shown in figure 2 together with two rotating coordinate systems xyz and XYZ. Both reference frames rotate about the Z axis at angular velocity Ω. In the xyz coordinate system, the z axis is

aligned along the long axis. In the XYZ coordinate system, the Z axis is vertical. The y and Y axes are identical. The principal moments of inertia of the egg about axes through G are taken as I_1, I_1 and I_3.

A. Angular momentum equations

As indicated in figures 1 and 2, the egg rotates about the z axis at angular velocity ω and simultaneously rotates about the Z axis at angular velocity Ω. These two components of the resultant angular velocity vector are the components that are measured experimentally. However, the angular momentum of the egg is best derived in terms of its components in the xyz coordinate system. In the latter system, the angular velocity of the egg is

$$\boldsymbol{\omega} = -\Omega \sin\theta\, \mathbf{i} + \frac{d\theta}{dt}\, \mathbf{j} + \omega_3\, \mathbf{k}\,, \tag{1}$$

where $\omega_3 = \omega + \Omega\cos\theta$, and the angular momentum of the egg is

$$\mathbf{L} = -I_1 \Omega \sin\theta\, \mathbf{i} + I_1 \frac{d\theta}{dt} \mathbf{j} + I_3\, \omega_3\, \mathbf{k}. \tag{2}$$

Alternatively, the angular velocity of the egg in the XYZ coordinate system is

$$\boldsymbol{\omega} = \omega \sin\theta\, \mathbf{I} + \frac{d\theta}{dt}\, \mathbf{J} + (\Omega + \omega\cos\theta)\, \mathbf{K}\,, \tag{3}$$

while the angular momentum in the XYZ coordinate system is

$$\mathbf{L} = L_X\, \mathbf{I} + L_Y\, \mathbf{J} + L_Z\, \mathbf{K}\,, \tag{4}$$

where $L_X = \sin\theta(I_3\omega_3 - I_1\Omega\cos\theta)$, $L_Y = I_1 d\theta/dt$ and $L_Z = (I_1\Omega\sin^2\theta + I_3\,\omega_3\cos\theta)$. Euler's angular momentum equation is given by

$$\frac{\partial \mathbf{L}}{\partial t} + \boldsymbol{\Omega} \times \mathbf{L} = \mathbf{X_P} \times (\mathbf{N} + \mathbf{F})\,, \tag{5}$$

where $\mathbf{X}_P$ is the vector distance from G (the center-of-mass) to P (the contact point), $\mathbf{N}$ is the vertical reaction force at P and $\mathbf{F}$ is the horizontal friction force at P. In the XYZ coordinate system, $\mathbf{X}_P = (-X_P,\, 0,\, -h)$, $\mathbf{N} = (0,\, 0,\, N)$ and $\mathbf{F} = (F_X,\, F_Y,\, 0)$, in which case equation (5) can be written in component form as

$$\frac{\partial L_X}{\partial t} - \Omega L_Y = F_Y h \tag{6}$$

$$\frac{\partial L_Y}{\partial t} + \Omega L_X = N X_P - F_X h \tag{7}$$

and

$$\frac{\partial L_Z}{\partial t} = -F_Y X_P \tag{8}$$

Each of the latter three equations indicates that there are three separates torques acting on the egg, each equation expressing the fact that the torque is equal to the rate of change of angular momentum. Only one of these equations is needed to describe steady precession of a spinning top or gyroscope, but all three are needed to describe both the precession and rise of a spinning egg. The terms ΩL_X and ΩL_Y correspond to the change in the angular momentum components due to precession about the vertical axis, a result that is familiar from the elementary theory of steady precession of a top or a gyroscope. The partial derivatives indicate simply that the magnitude of each angular momentum component can also change with time.

Equations (6) and (8) can also be written in the xyz coordinate system as [2, 14]

$$F_y z_P = -I_1 \sin\theta \, \frac{d\Omega}{dt} - (2I_1 \Omega \cos\theta - I_3 \, \omega_3) \frac{d\theta}{dt} \tag{9}$$

$$F_y \, r = I_3 \frac{d\omega_3}{dt} \tag{10}$$

where $F_y = F_Y$, and z_P and r are respectively the perpendicular distances from P to the x and z axes, as indicated in figure 2. Equation (9) indicates that the torque due to sliding or rolling friction, acting about the x axis, is equal to the rate of change of the angular momentum in the x direction. Equations (7) and (10) represent the corresponding rates of change of angular momentum in the y and z directions respectively.

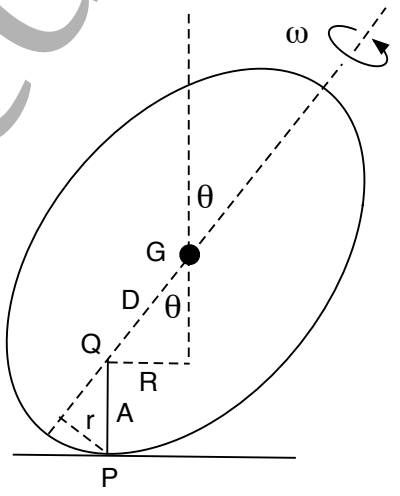

FIG. 3: Definition of the distances A, D, r and R.

The experiments described in Sec. III were undertaken with elliptical cross section spheroids rather than with eggs. The geometry is shown in figure 3. A vertical line from P intersects the long axis at point Q. PQ is of length A and QG is of length D. P is at distance $r = A\sin\theta$ from the axis while Q is displaced horizontally by distance $X_P = R = D\sin\theta$ from G. The distances h and z_P defined in figure 2 are given by $h = A + D\cos\theta$ and $z_P = D + A\cos\theta$. For a prolate spheroid of major radius a and minor radius b, $h^2 = a^2\cos^2\theta + b^2\sin^2\theta$ and $X_P = -dh/d\theta = (a^2 - b^2)\sin\theta\cos\theta/h$ [2,3].

B. Steady precession

Steady precession of a spheroid is described by equation (7) when θ remains constant in time, in which case $L_Y = 0$. If G rotates with radius B about the vertical precession axis, as indicated in figure 2, then the centripetal force $F_X = MB\Omega^2$, where M is the mass of the spheroid. Assuming also that $N = Mg$ while θ remains constant, we find that

$$\left[(I_1 - I_3)\cos\theta - \frac{MBh}{\sin\theta}\right]\Omega^2 - I_3\omega\,\Omega + \frac{MgX_P}{\sin\theta} = 0\,, \tag{11}$$

which is quadratic in Ω and therefore yields two different precession frequencies in general. For a spinning top, one of the two solutions is typically much less than ω, and corresponds to a relatively slow precession of the top. For a spinning speroid, Ω is much larger than ω at the start of the rise, but is comparable to ω after the spheroid rises. An essential feature of the solutions of equations (6)-(10) is that while the contact point slides on the horizontal surface, F_y remains positive and the spheroid rises. As the spheroid rises, ω increases and Ω decreases until the spheroid starts rolling, at which point the spheroid stops rising if F_y drops to zero. From then on, the spheroid undergoes steady precession. Alternatively, the spheroid will continue to rise at a slower rate if F_y decreases to small, finite value.

When a spheroid is spun rapidly it tends to precess about an axis through its center of mass, in which case $B = 0$. If it enters a rolling phase then $\omega = R\,\Omega/r = D\,\Omega/A$, in which case the precession frequency is given, from equation (11), by

$$\Omega^2 = \frac{MgD}{(I_3 D/A) - (I_1 - I_3)\cos\theta} \tag{12}$$

Unlike the case for a spinning top, the steady precession frequency of a spinning spheroid does not depend strongly on ω, and it does not depend strongly on the steady precession inclination angle, θ_S. For example, the steady precession frequency calculated for the S1

spheroid described below decreased from 49 rad/s to 40 rad/s as θ_S decreased from 89° to 2°. In the limit where $\theta \to 0$, equation (12) is not reliable since then $L_X \to 0$, $L_Y \to 0$, equations (6) and (7) are no longer relevant and neither is the rolling condition. When $\theta = 0$, a spheroid can rotate at an arbitrarily large rate, depending on the initial spin. By contrast, equation (12) indicates that Ω and ω approach limiting values as $\theta \to 0$.

3. Experimental method

Table 1: Properties of the three spheroids

No	Mass (g)	a (mm)	b (mm)	I_1 (kg.m^2)	I_3 (kg.m^2)
S1	132.1	29.95	19.98	3.42×10^{-5}	2.11×10^{-5}
S2	143.1	32.31	20.00	4.13×10^{-5}	2.29×10^{-5}
S3	128.7	35.95	18.00	4.16×10^{-5}	1.67×10^{-5}

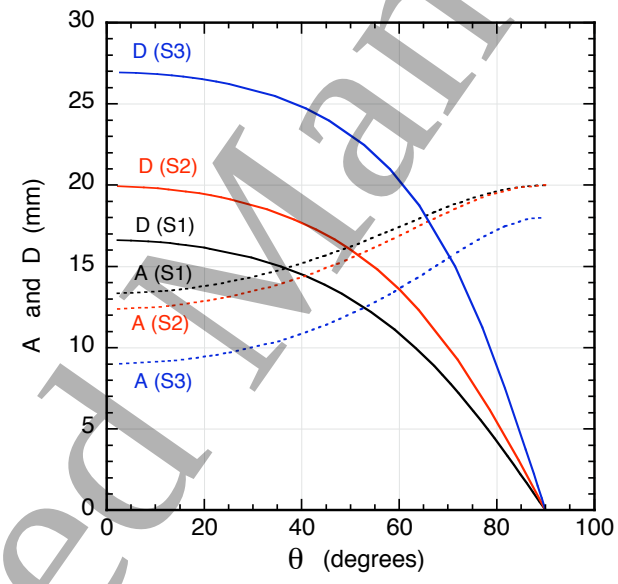

FIG. 4: Variation of A and D with θ for each of the three spheroids.

Most eggs, whether real, plastic or wood tend to be slightly asymmetrical in shape and are not ideally suited for accurate measurements of precession at high spin frequencies. Any asymmetry tends to introduce an undesirable wobble. For that reason, experiments were undertaken using three accurately machined aluminum spheroids with an elliptical cross-section. No other qualitative differences were found between spinning eggs and the spinning spheroids. The properties of each spheroid are shown in Table 1. If a and b are the major and minor radius respectively, then the mass $M = 4\pi ab^2\rho/3$, $I_1 = M(a^2 + b^2)/5$ and

$I_3 = 2Mb^2/5$, where ρ is the density. The measured mass and calculated volume indicates that $\rho = 2641 \pm 2\,\mathrm{kg/m^3}$ for each spheroid. The dimensions of each spheroid were different, resulting in differences in the geometrical distances A and D, as shown in figure 4. When a spheroid is horizontal, A is equal to the minor radius, b, and D is zero.

Each spheroid was spun on a smooth, horizontal table top and its motion was filmed with a Casio EX-F1 video camera at 300 fps or 600 fps viewing either above the spheroid or side-on. The video film was analysed with Tracker motion analysis software. Low spin frequency results were obtained by spinning each spheroid by hand. Higher spin frequencies were obtained using a circular nylon brush attached to a hand drill. The brush was pressed onto the spheroid when the spheroid was horizontal and the rotation frequency was increased to a desired value before lifting the brush vertically off the spheroid. Measurements were made of Ω, ω and the angle of inclination, θ, between the spin axis and the vertical, all as functions of time. The angular velocities were determined by marking each spheroid at various spots and recording the rotation angle of those marks from one frame to the next, or by recording the time taken for a given mark to rotate by one or more complete revolutions. All three quantities varied with time during any given precession cycle, by up to 30% in some cases, but those rapid variations were smoothed out by recording an average value for each precession cycle. Over a typical twenty second observation period, the spheroid precessed through about 100 revolutions. Each spheroid took about one second to reach its maximum height, the minimum angle θ varying from about 2° to about 60°, depending on the initial angular velocity.

When spinning an egg or any other object, it is difficult to avoid imparting translational motion as well. When filming the spheroids, the camera was zoomed in to enlarge the image, so any particular spin that was accompanied by a large horizontal velocity was automatically excluded from analysis since the spheroid disappeared from view before it had a chance to rise. However, the camera was zoomed out far enough to record its low frequency precessional motion as well as its high frequency precession.

The measured spins required careful interpretation. The angular velocity, ω, is defined in Sec. 2 as the spin about the long axis observed in a coordinate system rotating about the vertical axis at angular velocity Ω. The video camera was not rotated but remained fixed. Consequently, the observed spin in the laboratory frame of reference was $\omega_{Lab} = \omega + \Omega$. The spin, ω, was calculated by subtracting the measured precession frequency from ω_{Lab}.

Alternatively, ω could be determined in some cases by recording the position of a mark on the egg only after the egg rotated by one full precession cycle. In that manner, the fixed camera simulated a rotating camera recording only one frame each precession cycle.

4. Experimental results

A. Slow spin behaviour

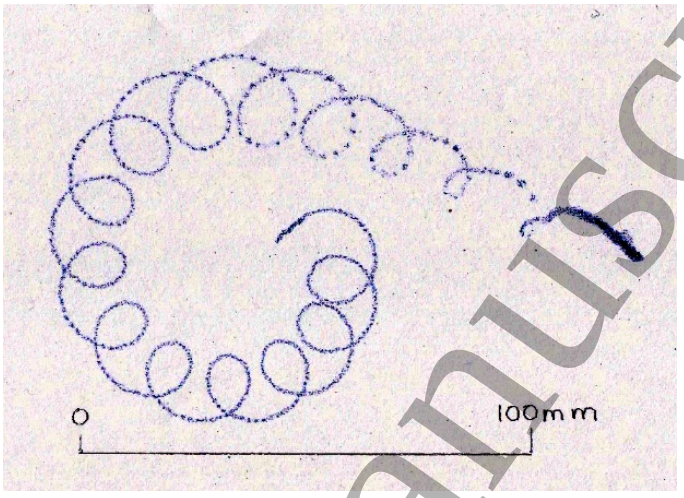

FIG. 5: A typical result showing the path of the contact point recorded by spinning S1 at relatively low speed on carbon paper. The spheroid was spun about a vertical axis by hand at the right, with $\theta \approx 90°$, and was lifted off the paper about 2 s later after it rose to $\theta \approx 40°$. The spheroid precessed about its center of mass at high frequency while simultaneously precessing in a large radius circular path at low frequency.

A spinning egg or spheroid tends to precess about two different vertical axes simultaneously. It precesses rapidly about a vertical axis passing through or close to its center of mass, and it also precesses slowly about a remote vertical axis. An example of the latter effect is shown in figure 5 where the path of the contact point on the table was made visible by allowing the spheroid to spin on carbon paper covering a sheet of white paper on the table. Slow precession is more obvious if the spheroid is spun at low speed since the spheroid then completes several large radius precession cycles while precessing rapidly in small radius loops. At high spin frequencies, the slow precession is not as obvious since the spheroid rises to a near vertical position quickly and then spins on the spot before it completes a large radius, slow precession cycle.

The path shown in figure 5 is defined by a sequence of closely spaced dots. Those dots indicate that the spheroid was jumping rapidly. The same effect was observed by rolling a billiard ball on carbon paper, the spacing between the dots being proportional to the rolling speed. It was concluded that the effect was due to surface roughness, causing the spheroid to jump by about 0.1 mm between each dot, rather than as a consequence of the dynamics of the spinning spheroid. Nevertheless, the spheroids were indeed observed on video film to jump occasionally by about 0.5 mm when spun at high speed, as reported previously [6, 7].

B. Steady precession results

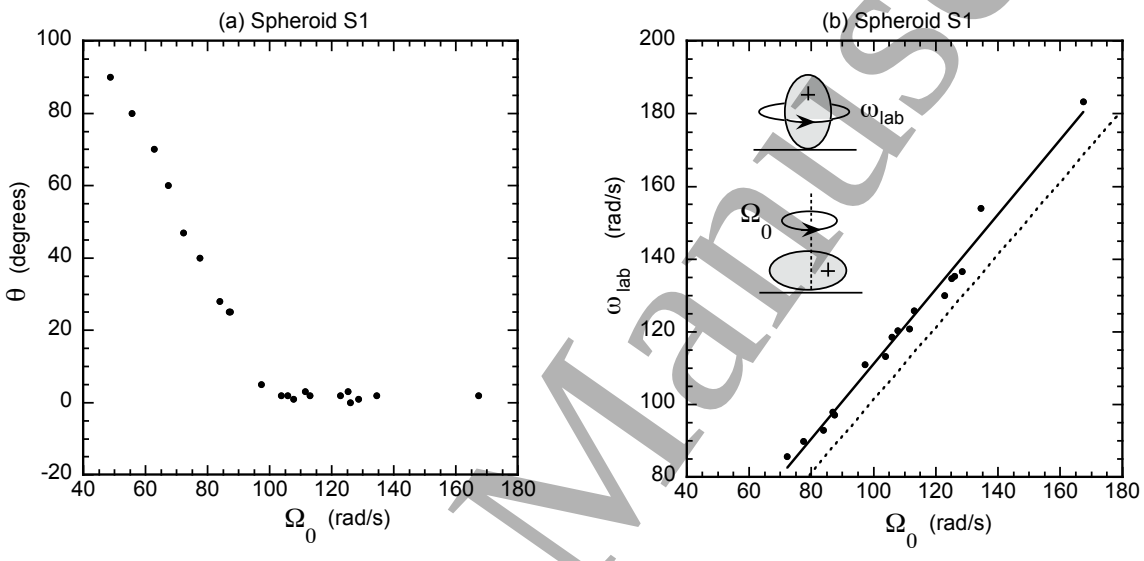

FIG. 6: Experimental results obtained with spheroid S1 showing (a) the angle of inclination, θ, when the spheroid rose to its maximum height, and (b) ω_{lab} at maximum height, both as a function of the initial precession frequency, Ω_0.

Each of the three spheroids behaved in a qualitatively similar manner, rising to an angle closer to the vertical as the initial rotation frequency was increased. Typical results for spheroid S1 are shown in figure 6. Figure 6(a) shows the angle of inclination of the long axis to the vertical, θ, at which the spheroid rose to its maximum height, as a function of the initial precession frequency, Ω_0. When Ω_0 was less than about 50 rad/s, the spheroid did not rise at all. When Ω_0 was greater than about 100 rad/s, the spheroid rose to an almost vertical position, the long axis being inclined less than two degrees from the vertical.

Figure 6(b) shows the corresponding spin about the long axis, ω_{lab}, as measured in the

laboratory frame of reference, after the spheroid rose to its maximum height. As indicated in figure 6(b), ω_{lab} was typically about 10 rad/s larger than Ω_0 in all cases for spheroid S1. As a result, there was a reduction in the angular momentum about the vertical axis as the spheroid rose, as expected from Eq. (8). Initially, $L_Z = I_1\Omega_0$. When the spheroid rises to $\theta = 0$, $L_Z = I_3\omega_{lab}$. For spheroid S1, I_1 was 62% larger than I_3, while Ω_0 was only slightly smaller than ω_{lab}.

C. Rise of each spheroid vs time

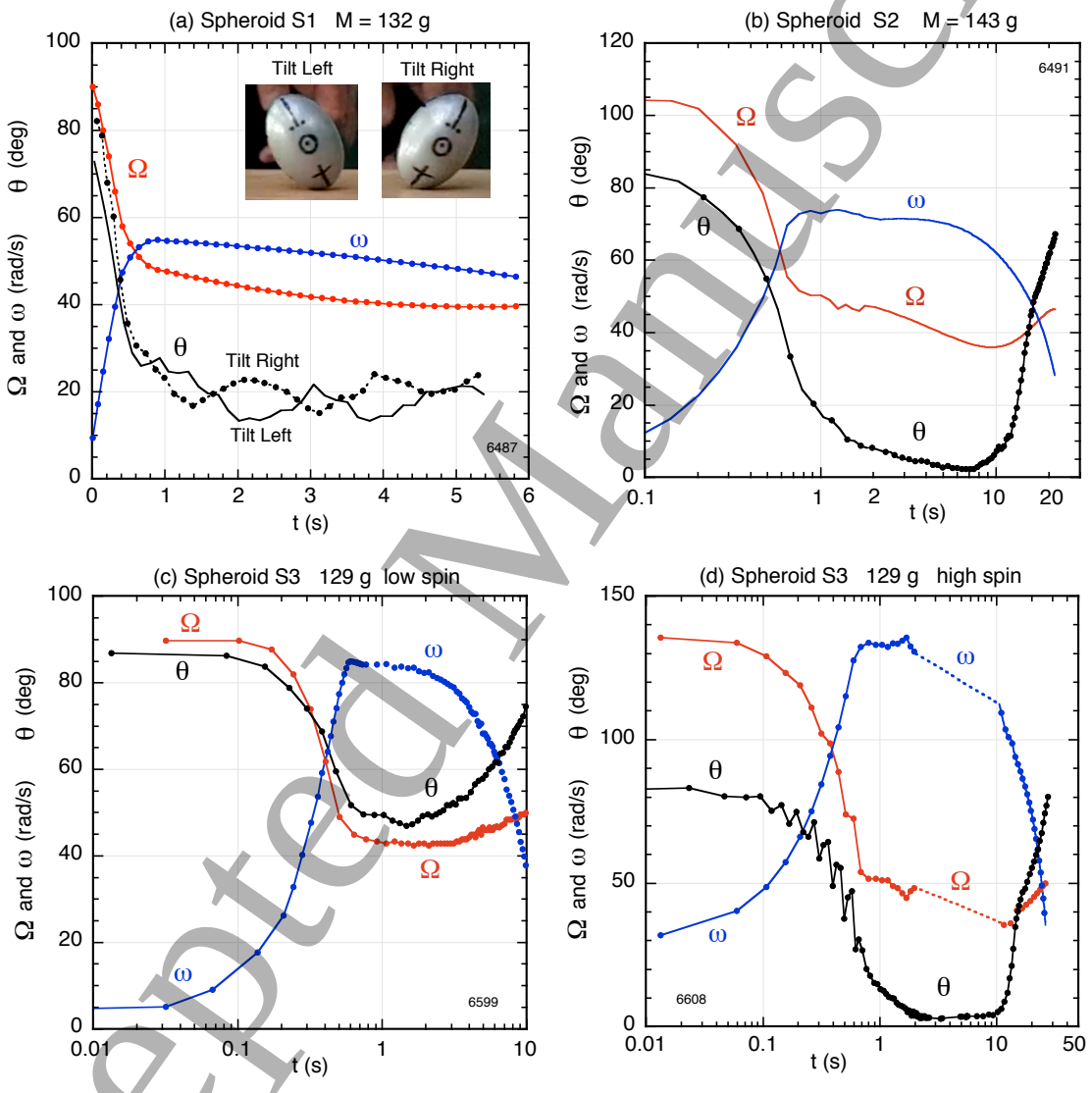

FIG. 7: Experimental results obtained with the three spheroids.

Measurements of Ω, ω and θ obtained with the three spheroids are shown in figure 7. All four results in figure 7 are qualitatively similar, in that each spheroid rose to its maximum

height in about 1.0 s, then precessed in a relatively steady manner for about ten seconds before falling slowly onto the horizontal surface over the next ten seconds. The relevant video film is shown in supplementary videos S1.mov, S2.mov, S3.mov and S4.mov. Specific differences are as follows:

In figure 7(a), spheriod S1 was spun at $\Omega_0 = 90$ rad/s and rose to within 20° of the vertical. It simultaneously precessed at 3.9 ± 0.4 rad/s in a large radius orbit by leaning inwards to the center of the orbit. As a result, the angle θ did not remain constant during each high frequency precession cycle, the spheroid tilting more to the left or to the right depending on the location of the spheroid along its large radius path. Two values of θ are therefore plotted in figure 7(a) during each high frequency precession cycle, one while the spheroid was tilted to the left, and one while it was tilted to the right. The precession frequency, Ω, shown in figure 7(a) is the high frequency value. The low frequency value (3.9 rad/s) is not plotted but the effect of the low frequency precession can be seen as a low frequency variation in θ when $t > 1$ s.

Figure 7(b) shows results for spheroid S2 spun at 105 rad/s. It rose quickly to within 20° of the vertical and then continued to rise slowly over the next seven seconds to within 2° of the vertical. Figures 7(c) and (d) show results for spheroid S3 spun at 90 and 135 rad/s respectively. This spheroid required a higher initial spin than the other two in order to rise to a near vertical position. After rising to its maximum height, the resulting spin, ω, was approximately equal to the initial precession frequency, Ω_0. By comparison, the maximum value of ω for the other two spheroids was significantly less than the initial precession frequency. The dashed straight line segments in figure 7(d) indicate that it was not possible to obtain an accurate measure of the precession frequency or the spin frequency, ω, when the spheroid was almost vertical. In the laboratory reference frame it was easy to measure the combined frequency $\omega + \Omega$, but not the separate components.

Numerical solutions of Eqs. (6) - (10) are shown in figure 8 in order to compare with the experimental results in figure 7. Each solution was obtained using the same initial starting values of ω, Ω and θ as those indicated in figure 6, and by assuming that the coefficients of sliding and rolling friction were 0.2 and 0.02 respectively. Sliding friction was also assumed to act in the X direction, with $F_X = \pm 0.2Mg$, depending on the direction of sliding along the X axis. It was assumed that motion of the center-of-mass in the X direction was negligible, in which case the direction of motion of the contact point along the X axis was taken to

depend on the sign of $d\theta/dt$. The primary effect of F_X was to damp rapid nutation of the spheroid. Alternatively, nutation in the numerical solutions can be eliminated by varying the initial starting conditions slightly. The effect of nutation can be seen in figure 8 as small oscillations in the θ and ω traces as the spheroids are rising, the nutation frequency being approximately equal to the precession frequency.

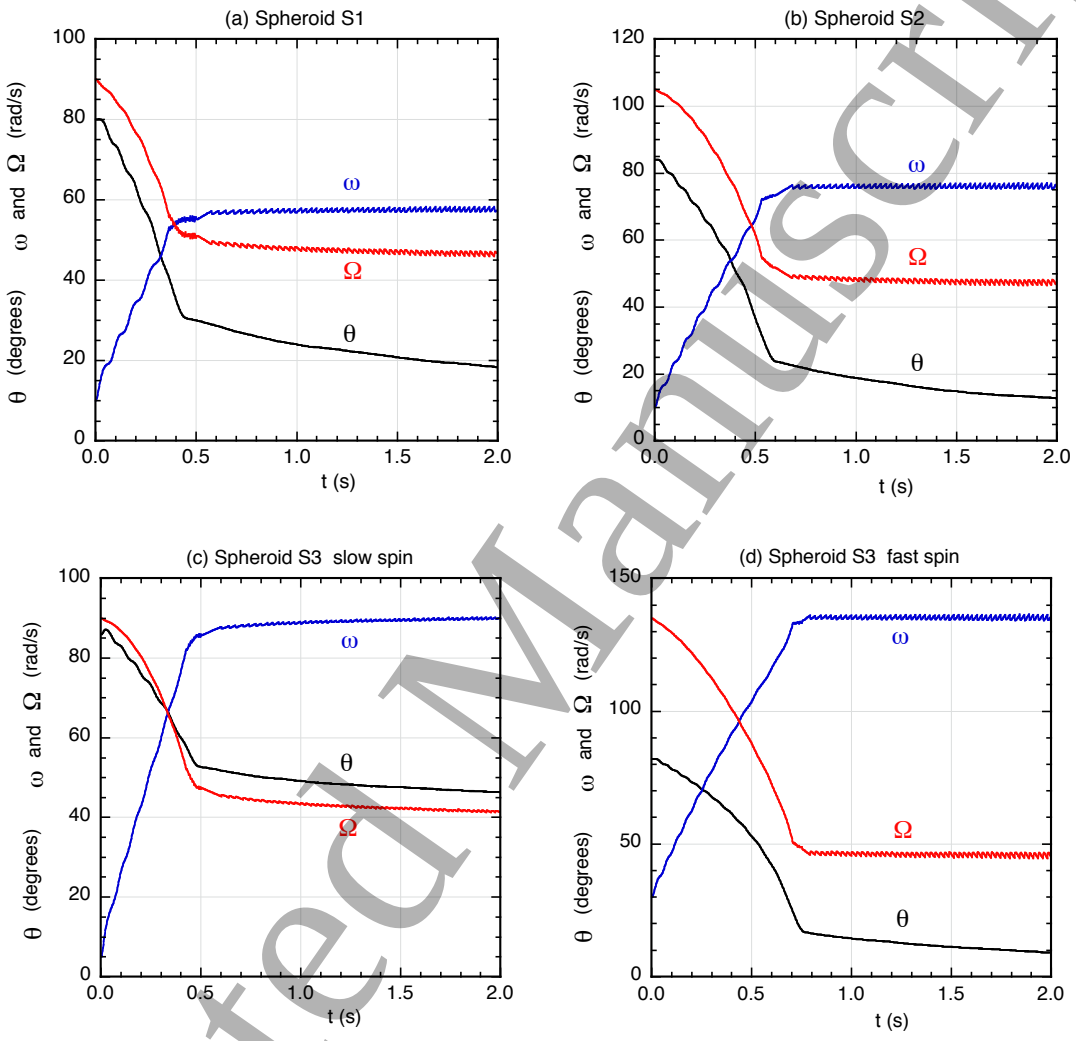

FIG. 8: Numerical solutions of equations (6)-(10) for the three spheroids.

The friction coefficients gave very good fits to the experimental data and were also consistent with the observed rate of change of ω_3, as indicated by equation (10). The calculations were terminated at $t = 2\,\mathrm{s}$ since it was clear that the subsequent behaviour of the spheroids was determined by rolling rather than sliding friction and since the experimental data were consistent with steady rolling precession as given by equation (12). The theoretical predic-

tions are compared with the experimental results in Table 2, by quoting values of ω, Ω and θ at $t = 2\,\mathrm{s}$. The agreement is sufficiently good that one can have confidence in both the experimental and the theoretical results and in quantities that can be derived from these results, as described in Section D.

Table 2: Comparison of experimental and theoretical results at $t = 2.0\,\mathrm{s}$

Result	ω (rad/s)		Ω (rad/s)		θ (degrees)	
figures 6, 7	Expt	Theory	Expt	Theory	Expt	Theory
(a)	54	57	45	46	19	18
(b)	72	75	47	47	8	13
(c)	84	90	43	42	50	47
(d)	133	135	48	46	5	10

D. Derived results

Results derived from the data in figure 7(a) are given in figure 9, showing (a) the two components of the angular velocity vector, ω_1 and ω_3 (b) the coefficient of friction, $\mu = F_y/(Mg)$, derived from equation (10) and the measured value of $d\omega_3/dt$, (c) the ratio $r\omega/R\Omega$, (d) the angle β between the angular momentum vector and the Z axis, (e) the Jellet constant $J = h\Omega$ and (f) the kinetic energy $\frac{1}{2}I_1\omega_1^2 + \frac{1}{2}I_3\omega_3^2$.

An obvious feature of all the results in figures 7 and 8 is the transition at $t \sim 0.5\,\mathrm{s}$ from a rapid to a gradual change in all variables. The transition is due to a change from sliding to rolling friction. As evidence for this effect, figure 9(c) shows the experimentally observed ratio $r\omega/(R\Omega)$ as a function of time. In addition, figure 9(b) shows the measured value of μ. The measured coefficient of sliding friction was approximately 0.2 for all four results shown in figure 7, so this value was chosen to calculate the results in figure 8. While $R\Omega$ remains larger than $r\omega$, the contact point P shown in figures 1-3 slides out of the page. Sliding friction acts to reduce Ω and to increase ω until $R\Omega = r\omega$, at which point the spheroid commences to roll. If the coefficient of rolling friction was zero, then the spheroid would stop rising. In fact, the spheroids in figure 7(b) and (d) were observed to rise slowly for several seconds after the rapid initial rise, indicating that the coefficient of rolling friction was small but not zero. The coefficient of rolling friction is typically less than 0.001 for hard surfaces, which suggests grip-slip rather than pure rolling behaviour after the spheroid stopped sliding.

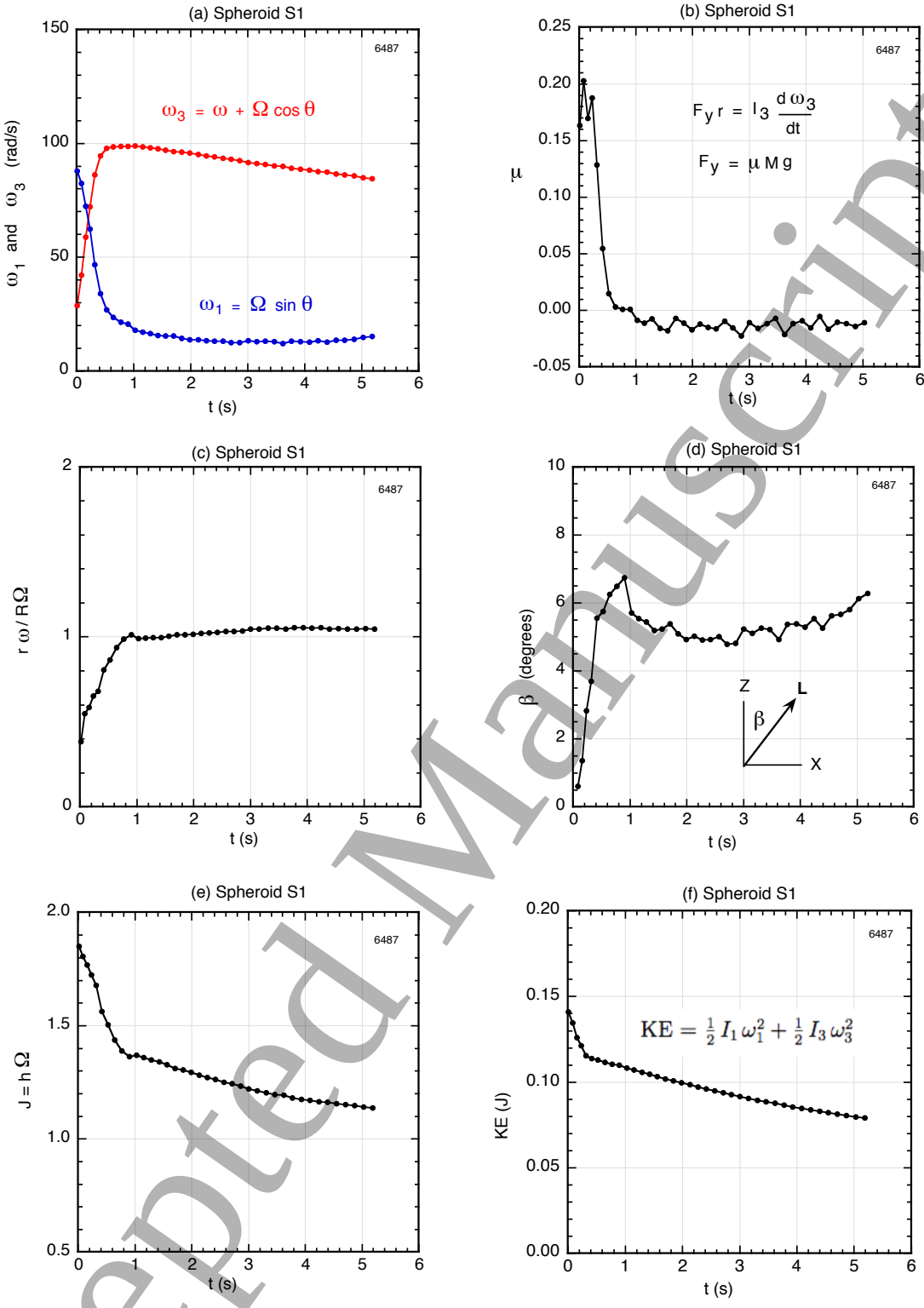

FIG. 9: Results derived from the experimental data for spheroid S1 shown in figure 7(a).

As noted in Sec. 1, the friction torque acts as shown in figure 1 to rotate the angular momentum vector away from the vertical as the spheroid rises. The rotation angle β shown in figure 9(d), defined by $\tan\beta = L_X/L_Z$, increased to about 6° before the spheroid started to roll and then remained relatively constant. Given that $\beta \ll \theta$ while the egg rises, then to a good approximation $\tan\theta = -L_x/L_z = I_1\Omega\sin\theta/I_3\omega_3$ from Eq. (2), so $\cos\theta \approx I_3\omega_3/(I_1\Omega)$. The latter relation provides an approximate estimate of the tilt angle while the egg rises and also provides a partial explanation for the rise. Since friction acts to increase ω_3 and to decrease Ω, θ must necessarily decrease, despite the fact that friction causes β to increase.

The Jellet constant $J = h\Omega$ (or the related quantity $I_1 h\Omega$) has been described by several authors [2, 3, 4, 19] as one of the important constants of motion for a spinning egg or tippe top. The significance of J is that if friction acts to reduce Ω then the egg will necessarily rise since h must increase. Moffatt and Shimomura [2] used the result that J is constant to explain the paradox of the rising egg. The result in figure 9(b) indicates that J decreased by 0.5 or by 27% as the egg rose. A similar reduction was found for the other three cases in figure 7.

Given the role played by sliding friction in causing the spheroid to rise, it is not surprising that the total energy decreases as the spheroid rises. The increase in potential energy was 0.012 J for spheroid S1, and the decrease in kinetic energy was 0.025 J during the rapid rise phase, as indicated in figure 9(f).

5. Discussion

It is clear from the experimental results that the sliding friction force, F_Y, plays a major role in determining the rise of a spinning egg (or spheroid) since the rate of rise decreases substantially when the egg enters a rolling (or grip-slip) mode. The role of F_Y can be understood by examining the three terms in equation (6). Numerical solutions indicate that all three terms are comparable in magnitude if the initial conditions are chosen somewhat arbitrarily, in which case strong nutation is observed, as shown in figure 10(a). However, it is possible to alter the initial conditions slightly to eliminate nutation, as indicated in figure 10(b). Nutation in the numerical solution shown in figure 10(a) is almost completely eliminated if the initial value of ω is taken as 7.8 rad/s rather than 10.0 rad/s, and if the initial rate of change in θ is taken as -1.5 rad/s. If nutation is eliminated in this way, it

becomes apparent that the $\partial L_X/\partial t$ term in equation (6) is about ten times smaller than the ΩL_Y term when the egg is rising steadily. It is only the high frequency components of $\partial L_X/\partial t$ and ΩL_Y, due to nutation, that are similar in magnitude. Rapid nutation has no significant effect on the slowly varying quantities shown in figure 10(b) which are also present in figure 10(a) as time average values of the rapidly varying terms.

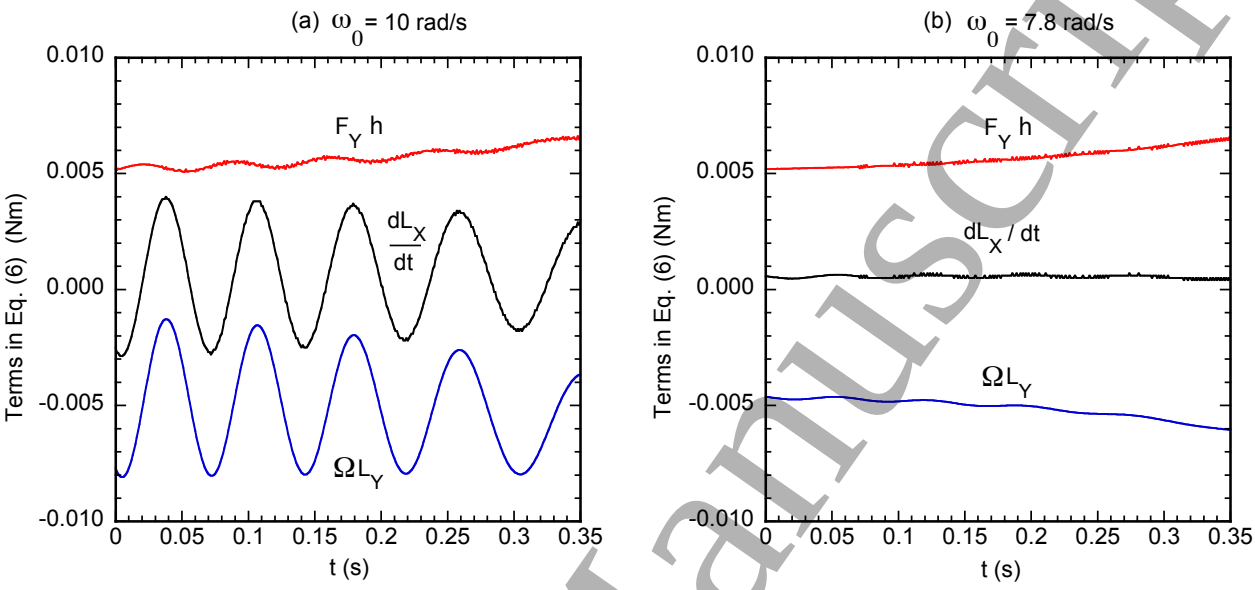

FIG. 10: The three terms in equation (6), (a) with nutation and (b) without nutation, for the same conditions as those in figure 8(a). In both cases, the initial precession frequency is 90 rad/s and the initial angle of elevation, θ, is 85°. However, the initial spin, ω_0, is 10 rad/s in (a) and 7.8 rad/s in (b). Nutation occurs at a frequency that is close to Ω, so the nutation frequency decreases as the spheroid rises and as Ω decreases.

The basic equation of motion describing the rise of an egg is therefore given to a good approximation by $F_Y h = -\Omega L_Y$, indicating that the torque in the X direction is equal to the rate of change of L_Y due to precession of the egg about the vertical axis. Since F_Y, h and Ω are all positive quantities, $L_Y = I_1 d\theta/dt$ is negative, meaning that the egg rises. The approximation that $L_X = 0$ is described in [2, 3] as the "gyroscopic balance approximation". The relation $L_Y = -F_Y h/\Omega$ accounts for the effect shown most clearly in figures 8(b) and 8(d) that a spinning egg rises slowly at first and then more rapidly as it approaches the rolling condition. Since $F_Y = \mu M g$ remains constant, L_Y increases in magnitude as h increases and as Ω decreases.

An analogous relation holds in the Y direction when the egg precesses at a steady rate, in

which case equation (7) reduces to $NX_P = \Omega L_X$, meaning that the torque in the Y direction is equal to the rate of change of L_X resulting from precession of the egg. The analogy can be extended by noting that the friction force in the Y direction causes the egg to rotate about the Y axis, while the normal reaction force in the Z direction sustains steady precession about the Z axis. Rotation about the Y axis is not sustained since F_Y decreases to a small value when the egg starts rolling. In a similar manner, rotation about the Z axis ceases if N is artificially decreased to zero. The latter effect was confirmed by filming a spinning top on a hand-held horizontal tray. When the tray was pulled down quickly, the top entered free fall. The top continued to spin about its long axis, but it stopped precessing about the vertical axis, as shown in supplementary video Free Fall.mov.

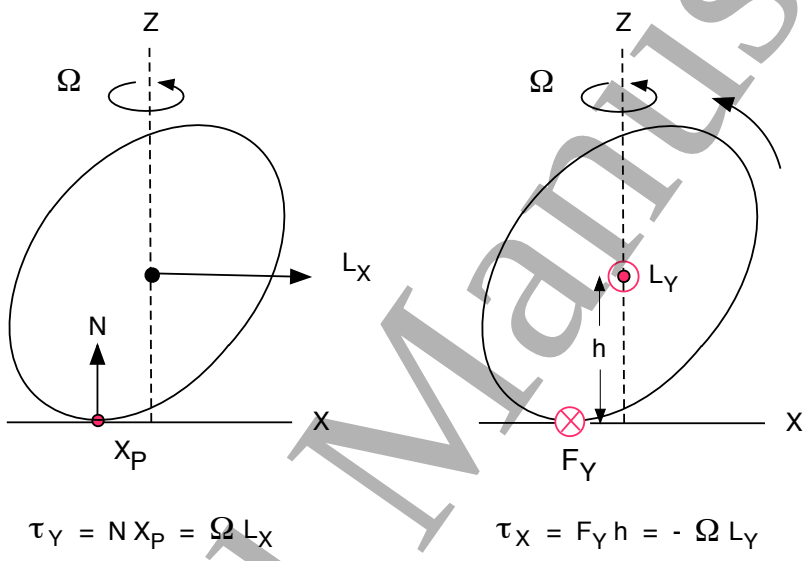

FIG. 11: The rise of a spinning egg is closely analogous to precession of the egg.

The close analogy between the two different effects is summarised in figure 11. The analogy is so close that one can conclude that the rise of a spinning egg is due to precession of the egg about the Y axis arising from the friction force in the Y direction, while steady precession of the egg about the Z axis arises from the normal reaction force in the Z direction. The initial rotation of the egg about the Z axis arises not from the normal reaction force but from the external torque applied about the Z axis when the egg is set in motion.

6. Conclusion

Experimental and theoretical results concerning the precession of spinning eggs are presented, showing that a spinning egg rises as a result of sliding friction. The results were

obtained with solid aluminium spheroids rather than eggs, but the basic physics can be expected to be the same. The friction force acts in a direction that increases the spin of the egg about its long axis and decreases the angular velocity of precession about the vertical axis. The friction force acts in the opposite direction to that of a spinning top since the precession frequency for an egg is initially much larger than the spin about the long axis. During the rapid rise, the angular momentum vector projected in the XZ plane rotates away from the vertical, unlike a simple spinning top. The sliding speed of the contact point decreases with time until the egg begins to roll, at which point the friction force drops substantially, the egg stops rising rapidly and the egg starts to precess about the vertical axis in a steady manner.

The rise of a spinning egg or a tippe top can be attributed to precession about the Y axis, arising from the friction force in the Y direction, in the same way that steady precession about the Z axis arises from the normal reaction force in the Z direction. Both effects are governed by equations of identical form, each indicating that the relevant torque due to the friction or normal reaction force is equal to the corresponding rate of change in the angular momentum arising from rotation about the vertical axis.

Acknowledgment

I am grateful to Professor Yutaka Shimomura from Keio University, Japan, for providing me with the three spheroids used in his own experiments and for sharing with me his insights into the physics of spinning eggs.

References

[1] Crabtree H 1909 *An Elementary Treatment of the Theory of Spinning Tops and Gyroscopic Motion* (Longmans Green, London, reprinted by Chelsea, 1967).

[2] Moffatt H K and Shimomura Y 2002 Spinning eggs - a paradox resolved *Nature* **416**, 385-386

[3] Moffatt H K, Shimomura Y and Branicki M 2004 Dynamics of an axisymmetric body spinning on a horizontal surface. I. Stability and the gyroscopic approximation *Proc. R. Soc. Lond. A* **460**, 36433672

[4] Sasaki K 2004 Spinning eggs - which end will rise? *Am. J. Phys.* **72**, 775-781

[5] Bou-Rabee N M, Marsden J E and Romero L A 2005 A geometric treatment of Jellett's egg *Z. Angew. Math. Mech.* **85**, 618 642

[6] Shimomura Y, Branicki M and Moffatt H K 2005 Dynamics of an axisymmetric body

spinning on a horizontal surface. II. Self-induced jumping *Proc. R. Soc. A 461* 17531774

[7] Mitsui T, Aihara K, Terayama C, Kobayashi H and Shimomura Y 2006 Can a spinning egg really jump? *Proc. Roy. Soc. A* **462**, 2897-2905

[8] Fokker A D 1941 The rising top, experimental evidence and theory *Physica* **8**, 591-596

[9] Fokker A D 1952 The tracks of top's pegs on the floor *Physica (Amsterdam)* **18**, 497-502

[10] Braams C M 1952 On the influence of friction on the motion of a top *Physica (Amsterdam)* **18**, 503-514

[11] Hugenholtz N M 1952 On tops rising by friction *Physica (Amsterdam)* **18**, 515-527

[12] Parkyn D G 1958 The Rising of Tops with Rounded Pegs *Physica (Amsterdam)* **24**, 313-330

[13] Deimel R F 1952 *Mechanics of the Gyroscope: the dynamics of rotation* (Dover, New York)

[14] Barger V and Olsson M 1994 *Classical Mechanics, A Modern Perspective* (McGraw-Hill, 2nd Ed.)

[15] Stefanini L 1979 Behaviour of a real top *Am. J. Phys.* **47**, 346-350

[16] Schonhammer K 1998 Elementary theoretical description of the heavy symmetric top *Am. J. Phys.* **66**, 1003-1007

[17] Pliskin W A 1954 The tippe top (topsy-turvy top) *Am. J. Phys.* **22**, 28-32

[18] Cohen R J 1977 The tippe top revisited *Am. J. Phys.* **45**, 12-17

[19] Gray C G and Nickel B G 2000 Constants of motion for nonslipping tippe tops and other tops with round pegs *Am. J. Phys.* **68**, 821-828

[20] Soodak H 2002 A geometric theory of rapidly spinning tops, tippe tops, and footballs *Am. J. Phys.* **70**, 815-828

[21] Cross R 2013 Spinning eggs and ballerinas *Phys. Ed.* **48** 51-55